

On the origin of ferromagnetism in oximato-based $[\text{Mn}_3\text{O}]^{7+}$ triangles

Joan Cano,^{*a,b,c} Thomas Cauchy,^a Eliseo Ruiz,^{a,b} Constantinos J. Milios,^d Constantinos C. Stoumpos,^f Theocharis C. Stamatatos,^{e,f} Spyros P. Perlepes,^{*f} George Christou^{*e} and Euan K. Brechin^{*d}

Received 3rd July 2007, Accepted 1st October 2007

First published as an Advance Article on the web 19th October 2007

DOI: 10.1039/b710055h

DFT calculations reveal the unusual ferromagnetic exchange observed in an oxo-centered Mn^{III} triangle may originate from a combination of the ‘non-planarity’ of the bridging oxime ligands and the non-parallel alignment of the Jahn–Teller axes.

Introduction

The fascinating observation of dominant ferromagnetic exchange interactions in a triangular $[\text{Mn}_3\text{O}]^{7+}$ complex¹ has led to much speculation over its origin. Such a metallic core is commonplace in $\text{Mn}(\text{III})$ carboxylate chemistry, exemplified by the well known class of compounds referred to as the ‘‘basic carboxylates’’ of general formula $[\text{Mn}^{\text{III}}_3\text{O}(\text{O}_2\text{CR})_6\text{L}_3]^+$ (where $\text{R} = \text{Me}, \text{Et}, \text{Ph}$ etc, and $\text{L} = \text{py}, \text{H}_2\text{O}$ etc.).² The magnetic interactions between the metal ions in this class of compounds have been studied for decades and in all cases are antiferromagnetic in nature, not only in the discrete trinuclear compounds, but also where the same $[\text{Mn}_3\text{O}]^{7+}$ unit is the basic building block of larger clusters.³ However, when three of the six carboxylates and the three pyridines in the complex $[\text{Mn}^{\text{III}}_3\text{O}(\text{O}_2\text{CMe})_6(\text{py})_3]^+$ are replaced with the oximato-based ligand mpko^{1-} ($\text{mpkoH} = \text{methyl-2-pyridyl ketone oxime}$) to give the complex $[\text{Mn}^{\text{III}}_3\text{O}(\text{mpko})_3(\text{O}_2\text{CMe})_3]^+$ (**1**, Fig. 1) the exchange is switched to ferromagnetic.¹ Initial inspection of the molecular structure of **1** prompted two possible reasons: (a) the central O^{2-} mediates antiferromagnetic exchange *via* $\text{M}_{\text{d}\pi} - \text{O}_{\text{p}\pi} - \text{M}_{\text{d}\pi}$ orbital overlap and the structural distortion which results in the central oxide being 0.295 Å above the $[\text{Mn}^{\text{III}}_3]$ plane (as opposed to exactly $(\pm 0.03\text{Å})$ in the $[\text{Mn}^{\text{III}}_3]$ plane in $[\text{Mn}^{\text{III}}_3\text{O}(\text{O}_2\text{CMe})_6(\text{py})_3]^+$ species) weakens the antiferromagnetic contribution to the observed exchange, J_{obs} , between the Mn ions. Since this J_{obs} is the sum of ferro- and antiferromagnetic contributions, and J_{obs} is in any case only weakly antiferromagnetic any structural distortion giving a non-planar $[\text{Mn}_3\text{O}]^{7+}$ core could lead to a ferromagnetic J_{obs} ; (b) the introduction of the two-atom oximato bridge ($\text{Mn}-\text{N}-\text{O}-\text{Mn}$) in place of the μ -carboxylate bridge and its non-planarity with respect to the $[\text{Mn}^{\text{III}}_3]$ plane tilts the balance such that the ferromagnetic contribution to J_{obs}

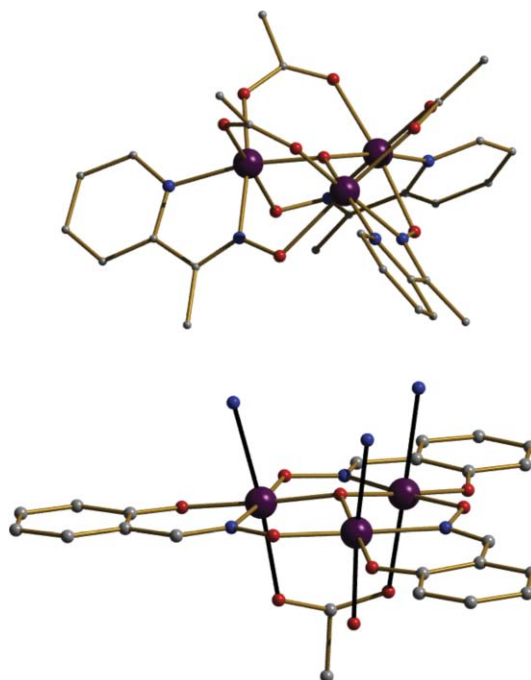


Fig. 1 The molecular structures of complexes **1** (top) and **2** (bottom). The C-atoms of the pyridines have been removed for clarity. Colour code: Mn, purple; O, red; N, blue; C, grey.

via the oximato ligands is now greater than the antiferromagnetic contribution *via* the oxide ion and carboxylates.

In order to attempt to answer this question we made the complexes $[\text{Mn}_3\text{O}(\text{sao})_3(\text{O}_2\text{CR})(\text{H}_2\text{O})(\text{py})_3]$ ($\text{R} = \text{Me}$ (**2**), Ph (**3**), $\text{saoH}_2 = \text{salicylaldoxime}$; Fig. 1).⁴ These complexes have very similar structures to **1**, with the central $\mu_3\text{-O}^{2-}$ ion 0.325 Å above the three Mn^{III} ions it bridges. The major differences come in the peripheral ligation where the sao^{2-} ligands, and hence the $\text{Mn}-\text{N}-\text{O}-\text{Mn}$ moieties, all now lie exactly on the $[\text{Mn}^{\text{III}}_3]$ plane, with the remaining carboxylates and solvent (pyridine) molecules lying perpendicular to the $[\text{Mn}^{\text{III}}_3]$ plane. The magnetic behaviour of **2** (and **3**) is indicative of dominant antiferromagnetic exchange between the metal centres (*vide infra*) resulting in an $S = 2$ ground state.⁴ This indicates that the non-planarity or ‘‘puckering’’ of the oximato ligands with respect to the $[\text{Mn}^{\text{III}}_3]$ plane is indeed an important factor in tilting the balance, as stated above, and giving the ferromagnetic exchange in complex **1**. This latter idea gains some credence when considering the

^aDepartament de Química Inorgànica and Institut de Recerca en Química Teòrica i Computacional (IQTC), Universitat de Barcelona, Diagonal 647, 08028, Barcelona, Spain. E-mail: joan.cano@qi.ub.es

^bInstitut de Nanociència i Nanotecnologia de la Universitat de Barcelona (IN2UB), Universitat de Barcelona, Diagonal 647, 08028, Barcelona, Spain

^cInstitució Catalana de Recerca i Estudis Avançats (ICREA), Spain

^dSchool of Chemistry, The University of Edinburgh, West Mains Road, Edinburgh, UK EH9 3JJ. E-mail: ebrechin@staffmail.ed.ac.uk

^eDepartment of Chemistry, University of Florida, Gainesville, FL, 32611-7200, USA. E-mail: christou@chem.ufl.edu

^fDepartment of Chemistry, University of Patras, 26504, Patras, Greece. E-mail: perlepes@patreas.upatras.gr

magnetic behaviour displayed by the two related hexanuclear complexes $[\text{Mn}^{\text{III}}_6\text{O}_2(\text{sao})_6(\text{O}_2\text{CR})_2(\text{R}'\text{OH})_4]$ (**4**) and $[\text{Mn}^{\text{III}}_6\text{O}_2(\text{Et-sao})_6(\text{O}_2\text{CR})_2(\text{R}'\text{OH})_4(\text{H}_2\text{O})_2]$ (**5**) (where R and R' = H, Me, Et *etc*; saoH_2 = salicyldoxime, Et-saoH₂ = 2-hydroxyphenylpropanone oxime).⁵ Both **4** and **5** have structures containing two (linked) oximate-bridged $[\text{Mn}_3\text{O}]^{7+}$ triangles analogous to those present in **2** and **3**, with the only major structural difference between the two originating from the severe twisting of the Mn–N–O–Mn moieties within each Mn₃ sub-unit caused by the presence of the bulkier Et-substituent. This is evidenced by the average Mn–N–O–Mn torsion angle, which in **4** is $\alpha_v = 17.5^\circ$ compared to $\alpha_v = 36.5^\circ$ for **5**. Magnetically, however, their properties are remarkably different with complex **4** displaying a spin ground state of $S = 4$ as a result of ferromagnetic exchange between the two antiferromagnetically coupled $[\text{Mn}^{\text{III}}_3]$ triangles, whilst complex **5** displays an $S = 12$ ground state as a result of dominant ferromagnetic exchange.⁵ Here we present DFT calculations performed on complexes **1–3** that suggest the oximate group twist and the non-parallel alignment of the Jahn–Teller axes are contributors that cause the final change in J and the ferromagnetic exchange in the $[\text{Mn}_3\text{O}]^{7+}$ unit of **1**. This is our first attempt at understanding the matter theoretically.

Computational details

All theoretical calculations were carried out with the hybrid B3LYP method,^{6–8} as implemented in the Gaussian03 program.⁹ A quadratic convergence method was employed to determine the most stable wave functions in the SCF process.¹⁰ Double- ζ and triple- ζ quality basis sets proposed by Ahlrichs and co-workers have been used for non-metal and metal atoms, respectively.^{11,12} In some calculations, triple- ζ quality basis sets were used for all atoms—these produced very similar results to that obtained using mixed basis sets. The electronic configurations used as starting points were created using Jaguar 6.0 software.¹³ The approach employed herein to determine the exchange coupling constants (for polynuclear complexes) has been described in detail elsewhere.^{14–16} To evaluate three J constants for complex **1**, assuming a non symmetrical structure, an $S = 6$ spin configuration $\{+,+,+\}$ and three $S = 2$ $\{-,+,\}$, $\{+,-,\}$ and $\{+,-,-\}$ configurations (where positive and negative signs indicate ‘spin-up’ and ‘spin-down’, respectively) were employed. The $\{+,-,-\}$ spin configuration has not been considered for the calculation of the two J values in **2** and **3** due to their symmetry. The SIESTA program (Spanish Initiative for Electronic Simulations with Thousands of Atoms)^{17–20} was employed with the GGA exchange–correlation functional proposed by Perdew, Burke and Ernzerhof (PBE) for additional electronic calculations.²¹ We have selected values of 50 meV for the energy shift and 200 Ry for the mesh cut-off that provide a good compromise between accuracy and the computer time required to calculate the exchange coupling constants.^{22,23} Only external electrons have been included in the calculations, the cores being replaced by norm-conserving scalar relativistic pseudopotentials factorized in the Kleinman–Bylander form.²⁴ These pseudopotentials have been generated following the approach proposed by Trouiller and Martins²⁵ from the ground state atomic configurations of all the atoms except for Mn, for which the Mn^{II} configuration $[\text{Ne}]3s^23p^64s^03d^5$ was employed. The core radii for the s, p and d components of the Mn atoms are

1.4, 1.9 and 1.5, respectively, and we have included partial-core corrections for a better description of the core regions.²⁶ The cut-off radii were 1.15 for oxygen, nitrogen and hydrogen atoms, 1.25 for carbon, and 1.6 for chlorine, respectively.

Discussion

Magnetic measurements

Solid state dc magnetization measurements were performed on the three studied complexes (**1–3**) in the temperature range 5–300 K in a field of 1.0 kG. Complex **1** displays an increase in the $\chi_M T$ value when cooled, and a value close to that expected for a $S = 6$ spin state is reached at low temperature, indicative of ferromagnetic exchange between the three Mn^{III} ions (Fig. 2a).¹ For complexes **2** and **3**, the room temperature $\chi_M T$ values of approximately 8.5 and 7.5 cm³ K mol^{−1}, respectively are slightly lower than that expected for three non-interacting Mn^{III} centres (9.0 cm³ K mol^{−1} for $g = 2.0$; Fig. 2b–c). As the temperature is lowered the value of $\chi_M T$ drops very gradually reaching values of 2.82 and 2.72 cm³ K mol^{−1} at 5 K for **2** and **3**, respectively. These values are close to that expected for an $S = 2$ spin ground state (3.0 cm³ K mol^{−1} for $g = 2.0$), and are indicative of relatively weak antiferromagnetic exchange between the Mn^{III} ions. The sharp decrease in the value of $\chi_M T$ at low temperatures ($T < 10$ K) in all three compounds is assigned to the presence of intermolecular antiferromagnetic interactions, Zeeman effects and/or zero-field splitting.

Two different magnetic exchange pathways, J_i , coexist in **1–3** (Fig. 3): (i) the first is mediated by an oximate (μ -NO), an oxo (μ -O) and a carboxylato (μ -O₂CR) group (J_a); (ii) the second is similar to J_a but minus the bridging carboxylate ligand (J_b) and appears only in **2** and **3**. To analyse the experimental data and from the phenomenological Heisenberg spin Hamiltonian

$$\hat{H} = -J_a \hat{S}_1 \cdot \hat{S}_2 - J_b (\hat{S}_1 \cdot \hat{S}_3 + \hat{S}_2 \cdot \hat{S}_3)$$

we have deduced a quantum theoretical law by means of the vector coupling (Kambe) model. In order to simplify some equations a global energy shift has been performed, so the energy of the different states S_T can be expressed as follows:

$$E(S_A, S_T) = -\frac{(J_a - J_b)}{2} S_A (S_A + 1) - \frac{J_b}{2} S_T (S_T + 1)$$

where S_T and S_A correspond to the total spin and intermediate spin of a particular molecular spin state deduced from the operators: $\hat{S}_A = \hat{S}_1 + \hat{S}_2$ and $\hat{S}_T = \hat{S}_3 + \hat{S}_A$. For **1**, the presence of the same bridging ligands for all three interactions allows us to assume that $J_a = J_b$ (this fact has been corroborated by theoretical calculations, *vide infra*). Least squares fitting (300–50 K) gives $J_a = +20.0 \pm 0.6$ cm^{−1} and $g = 1.991 \pm 0.005$. In order to reproduce the experimental measurements at low temperatures, we have introduced a parameter (D) that describes the local axial magnetic anisotropy of the Mn^{III} ions. This leads to the appearance of several local minima in the fitting process, the most stable of which corresponds to $D = -5.5$ cm^{−1}, with the values of the remaining parameters being slightly modified: $g = 2.005$ and $J_a = +18.1$ cm^{−1}. The obtained D parameter is consistent with published literature values, if a little high.

Assuming an antiferromagnetic J_b exchange coupling, an $S = 2$ spin ground state is only possible for **2** and **3** when the J_a/J_b

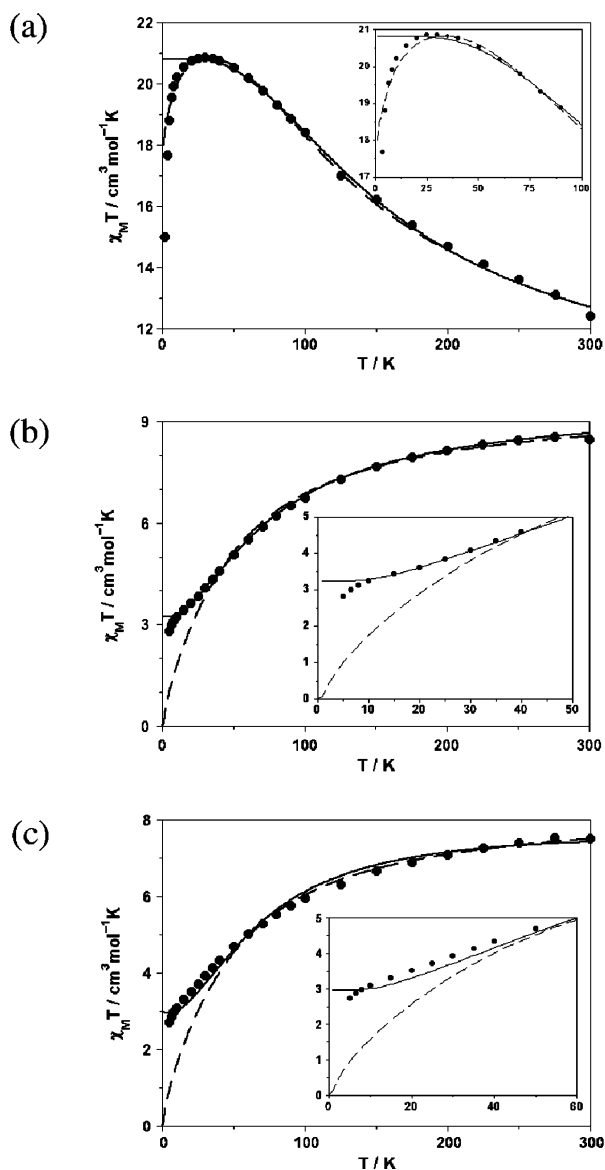


Fig. 2 Plot of $\chi_M T$ vs. T for the complexes **1** (a), **2** (b) and **3** (c). Enlargements of the lowest temperature regions are shown in the insets. The solid lines correspond to fits of the experimental data. The dashed lines correspond to: in **1**, the best fit including a parameter (D) for the local axial magnetic anisotropy of the Mn^{III} ions; and, in **2** and **3**, the best fits at higher temperatures including several restrictions to the values of the exchange coupling constants.

ratio is placed in the interval $[-\infty, -2]$. However, this interval is wider ($[-\infty, 0]$) when ferromagnetic J_b constants are considered. For $J_b = 0$, the quintet ground state is degenerate with S states ranging from 3 to 6. The best fits for **2** and **3** (Fig. 2b and 2c, respectively) were obtained for the following parameters (300–10 K): $J_a = +4.0 \pm 1.8 \text{ cm}^{-1}$, $J_b = -10.4 \pm 0.5 \text{ cm}^{-1}$ and $g = 2.075 \pm 0.007$ for **2** and $J_a = +4 \pm 10 \text{ cm}^{-1}$ and $J_b = -10 \pm 3 \text{ cm}^{-1}$ and $g = 1.99 \pm 0.03$ for **3** (Fig. 2) corresponding to an $S = 2$ spin ground state. The agreement factor of the fit, defined as $F = \left\{ \sum [\chi_{\text{expt}}^i - \chi_{\text{calcd}}^i]^2 \right\} / \left\{ \sum [\chi_{\text{calcd}}^i]^2 \right\}$ is reasonably good for **1** and **2** ($F = 4.6 \times 10^{-5}$ and 1.3×10^{-5} , respectively) and fair for **3** ($F = 5.5 \times 10^{-4}$). These results show that the strongest

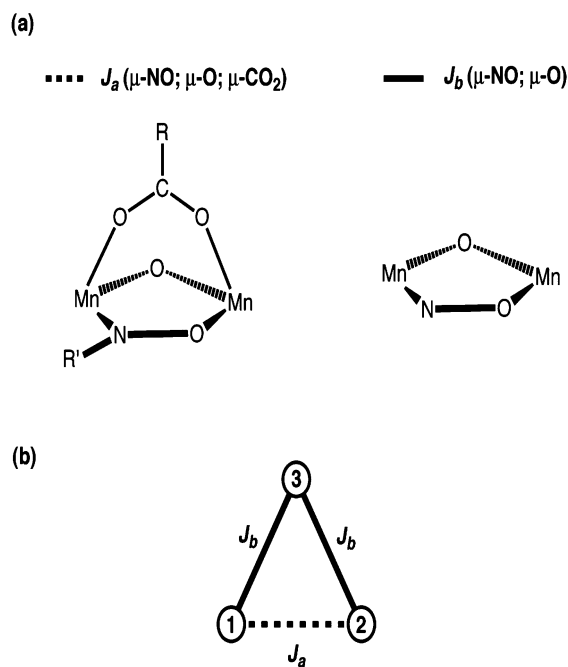


Fig. 3 (a) Schematic view of the two different exchange pathways and (b) topologies of magnetic interaction in **2** and **3**. In complex **1**, the two exchange couplings J_b and J_a are equivalent.

exchange coupling (J_b) hinders a good evaluation of the weaker ferromagnetic coupling (J_a), especially in the case of complex **3**. Despite this difficulty, the obtained values are the only ones that are able to perfectly reproduce the dependence of the magnetic susceptibility. Complexes **2** and **3** display similar values for J_a and J_b , as expected from their structural similarity. We again introduced a D parameter to describe the local axial magnetic anisotropy of the Mn^{III} ions, but the results obtained were dependent upon the starting point values in the fitting process. In order to overcome this problem we fixed all parameters to the values obtained in the previous fits, and allowed only the optimization of D . The values so obtained for D (-3.2 and -3.4 cm^{-1} for **2** and **3**, respectively) are in excellent agreement with those found in the literature.

From the results obtained from the fitting of the magnetic data some initial observations can be made: (i) the exchange coupling mediated by the three different bridging ligands (J_a) oximato, oxo and carboxylato) is ferromagnetic, but becomes antiferromagnetic (J_b) when the carboxylate ligand is not present; (ii) the J exchange coupling constant appears to be independent of the nature of the carboxylate present (*i.e.* acetate *versus* benzoate), as reflected in the similar values obtained for complexes **2** and **3**; (iii) the fitted J_a value for **1** is very different to those obtained for **2** and **3**.

In order to explain these observations, to analyze the role of the structural differences between the three complexes, and the possible presence of an orbital countercomplementarity phenomenon, electronic calculations based on density functional theory have been performed.

Theoretical calculations

Theoretical calculations based on Density Functional Theory have been performed using the full crystal structures of **1–3**. The crystal

structures of **2** and **3** show a structural disorder involving the μ -carboxylate group and a coordinated water molecule such that these groups are shared by the three Mn^{III} ions and an average of their atomic positions is obtained. In our calculations the water molecule is restrained to be coordinated to only one of the metal cations and likewise the carboxylate group acts only as a bridging ligand between the other two manganese ions. Complex **1** shows no structural disorder resulting in the presence of three “equivalent” Mn^{III} ions with the same bridging groups between each pair of Mn^{III} ions. We have, however, still calculated three J values to check if they are truly equivalent.

The calculated J constants are collected in Table 1. A first glance allows us to extract some initial conclusions: (i) the values obtained using the numerical basis set and PBE functional provide larger J values than those obtained with the Gaussian basis set and the hybrid B3LYP functional; (ii) the three calculated J values for complex **1** are very similar. Thus, we can consider it an acceptable approximation to employ only one J value in the fitting procedure; (iii) the calculated J values show a good agreement with those obtained experimentally—with the exception of J_a in complexes **2** and **3**, where a weak antiferromagnetic interaction is obtained rather than the ferromagnetic interaction obtained from the fitting of the experimental data; (iv) complexes **2** and **3** present very similar J values independently of the presence of PhCO_2^- or MeCO_2^- groups, as was found experimentally. *i.e.* a different carboxylate ligand appears not to introduce important changes to the exchange couplings. This is most likely due to the large Mn–O bond distances directed by the Jahn–Teller distorted Mn^{III} ions.

In order to analyze why we obtained the ‘wrong sign’ for the J_a interaction we have explored the dependence of the J value with the change in conformation of the carboxylate and water ligands. This has been achieved by performing a geometrical optimization of these ligands (on complex **2**) while fixing the positions of all other atoms. For such partially optimized geometry, J_a values of -0.8 and $+1.0 \text{ cm}^{-1}$ are obtained with the B3LYP and PBE

approaches, respectively, while the J_b value remains essentially unchanged (-6.5 and -7.8 cm^{-1}). These results indicate a large dependence of the calculated J_a values with the disposition of the carboxylate and water ligands. Consequently, the presence of disorder in their atomic positions does not allow for a rigorous estimation of J_a . It is worth noting, however, that these calculated J_a values are similar to those fitted by Chaudhuri *et al.*²⁷ for the wing-body interaction of two Mn_4 butterfly complexes (-0.94 and -3.26 cm^{-1}) with similar bridging ligands. We would also like to comment that the J_a values estimated by DFT calculations (even if they are of the ‘wrong sign’) are able to reproduce the experimental curves considering low values for the g -factor. Thus, when the temperature range 300–35 K (300–50 for **3**) is considered, values for J_a and J_b similar to those obtained in the previous fit are found. A perfect agreement between the theoretical and experimental $\chi_{\text{M}} T$ vs. T curves (Fig. 2b) is found when the J_a/J_b ratio is replaced by the value found by DFT calculations (0.812 and 0.783 for **2** and **3**) and kept constant. In this case, the fitting process estimates values for the exchange coupling constants ($J_a = -5.13 \pm 0.13 \text{ cm}^{-1}$, $J_b = -6.32 \pm 0.18 \text{ cm}^{-1}$ ($g = 2.066 \pm 0.009$) and $J_a = -4.93 \pm 0.13 \text{ cm}^{-1}$, $J_b = -6.29 \pm 0.18 \text{ cm}^{-1}$ ($g = 1.932 \pm 0.007$) for **2** and **3**, respectively) very close to the theoretical ones. At lower temperatures the theoretical and experimental curves diverge.

At this stage, some questions regarding the exchange coupling constants of the studied complexes remain unanswered: why do the J_a and J_b exchange constants have opposite signs in complexes **2** and **3** compared to complex **1**, and why is the J_a exchange in **1** ferromagnetic with a coupling constant considerably stronger than that found in **2** and **3** with the same bridging ligands?

To answer the first question, we have performed calculations with a partially optimized model of **2**, replacing the carboxylate ligand with two water molecules. These B3LYP calculations provide the same value of -6.6 cm^{-1} for J_a and J_b suggesting that, despite the small differences between J_a and J_b in **2**, the reason for the weaker antiferromagnetic or even ferromagnetic value of J_a when the carboxylate bridging ligand is present may be due to a countercomplementarity effect.^{28,29} Ferromagnetism is favoured by the presence of a small energy gap between the orbitals bearing the unpaired electrons (SOMOs)—as proposed by Hay–Thibeault–Hoffman.³⁰ Thus, sometimes ferromagnetic behaviour appears due to the presence of bridging ligands that induce opposite effects on the SOMOs energies resulting in a small total energy gap; such an effect is usually referred to as ‘countercomplementarity’. For instance, the oxo and oximate bridging ligands give an orbital order showing a more stable symmetric SOMO, while the carboxylate ligand favours the stability of the antisymmetric orbital (Fig. 4). Thus, the combination of these three bridging ligands in complexes **2** and **3** results in a small energy gap between SOMOs and ferromagnetic or weak antiferromagnetic coupling. When the carboxylate ligand is absent, the oxo and oximate ligand produce an antiferromagnetic interaction. In agreement with these theoretical results is our recent work on the related Mn_6 complexes with oxo and oximate bridging ligands that display antiferromagnetic coupling.⁵ This phenomenon has been analysed exclusively for the z^2 magnetic orbital. However, there are other additional contributions supplied by the t_{2g} magnetic orbitals that can mask or weaken the countercomplementarity phenomenon—but the exchange couplings from t_{2g} orbitals are usually less important than those where e_g orbitals are involved. It is also worth

Table 1 Exchange coupling constants (J_a and J_b , in cm^{-1}) calculated for complexes **1–3** with the PBE functional and the SIESTA code and with the B3LYP functional and the Gaussian program (see Computational details section) and ground spin state (S_{GS}). Experimental fitted data is provided for comparison

	Bridging ligands	PBE	B3LYP	Exp.	S_{GS}
Complex 1					6
J_a	$\mu_3\text{-O}$, $\mu\text{-NO}$, $\mu\text{-O}_2\text{CMe}$	+43.3 ^a	+14.4 ^b	+20.0	
Complex 2					0
J_a	$\mu_3\text{-O}$, $\mu\text{-NO}$, $\mu\text{-O}_2\text{CMe}$	-6.7	-5.6	+4.0	
J_b	$\mu_3\text{-O}$, $\mu\text{-NO}$	-9.1	-6.9	-10.4	
Complex 3					0
J_a	$\mu_3\text{-O}$, $\mu\text{-NO}$, $\mu\text{-O}_2\text{CPh}$	-7.0	-5.4	+4	
J_b	$\mu_3\text{-O}$, $\mu\text{-NO}$	-9.4	-6.9	-10	

^a Average of +40.8, +43.8 and +45.4 cm^{-1} (Mn...Mn distances 3.188, 3.201 and 3.191 Å, respectively) ^b Average of +13.8, +15.3 and +14.2 cm^{-1} (Mn...Mn distances, 3.188, 3.201 and 3.191 Å, respectively).

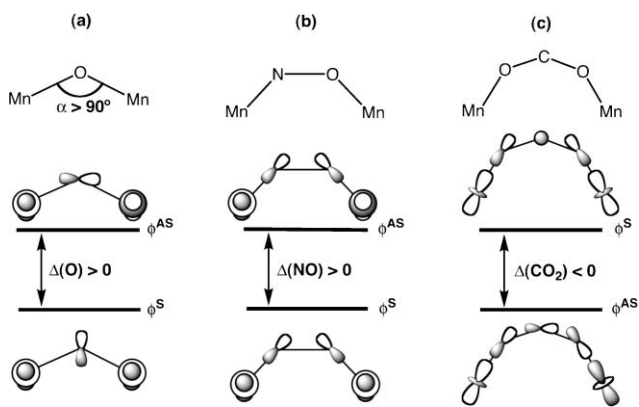


Fig. 4 Energy gaps and order of the SOMOs (AS, antisymmetric and S, symmetric combinations) corresponding to the z^2 magnetic orbitals with oxo (a), oximate (b) and carboxylate (c) bridging ligands.

noting that the oxo bridging ligand enhances the energy difference for large Mn–O–Mn angles and diminishes the difference for small Mn–O–Mn angles.

One might argue against this conclusion at this point by considering that the t_{2g} orbital pathways are not insignificant. For example, the countercomplementarity effect is dominant in copper(II) dimers³¹ where there is only one magnetic orbital (a σ one) and so the countercomplementarity involving this is the almost sole controller of J . If we accept that the t_{2g} pathways cannot be ignored, then we cannot avoid suggesting that overlaps with the central oxo ligand play some role and thus also its displacement from the Mn_3 plane since that affects them. Another point of discussion could be the change in J sign upon the $MeCO_2^-$ versus H_2O switch in **2**. The absolute change is only a few cm^{-1} and this could be due to the anionic versus neutral nature of the ligands, their small differences in Mn–O bond lengths and their effect on the energies of the $Mn^{III} t_{2g}$ and e_g magnetic orbitals, which will change the overlaps and thus the J_{AF} and J_F contributions. However, one would expect these effects to be small.

For complex **1**, the exchange coupling remains ferromagnetic ($+31\text{ cm}^{-1}$) if the carboxylate bridging ligands are replaced by water molecules. This result rules out the presence of a similar countercomplementarity effect and suggests an alternative origin for the ferromagnetism. Analysis of the coordination of the Mn^{III} cations in **1–3** reveals two important differences: (i) the presence of a structural distortion that breaks the co-planarity between the coordination planes involving the oximate and oxo bridging ligands in the $\{Mn_2O(NO)\}$ unit (average τ of 29.2° in **1**; and $\tau = 18^\circ$ and 17° in **2** and **3**, respectively, Fig. 5); and (ii) a non-parallel orientation of the Jahn–Teller axes in **1** and a near-parallel orientation of the Jahn–Teller axes in **2** and **3** (perpendicular to the Mn_3 plane (Fig. 5)).

In order to check if these structural differences are responsible for the differences in J_a , we have generated and analysed the parameter changes in analogous dinuclear model complexes. Dinuclear models are employed because trinuclear structures would produce large variations in the τ angle mediating important changes in bond distances and angles. The calculated J values (not shown) for dinuclear models of complex **1** indicate a considerable reduction in the strength of the ferromagnetic interaction when the τ angle decreases. Likewise, the non-parallel arrangement of

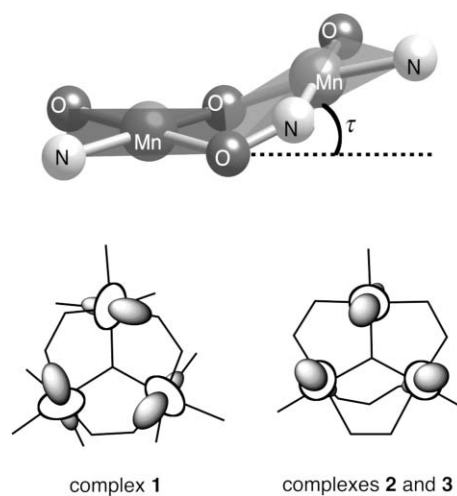


Fig. 5 Scheme of the structural distortion of the $\{Mn_2O(NO)\}$ unit (top), and the spatial orientation of the Jahn–Teller axes in complexes **1–3**.

the Jahn–Teller axes in **1** provides a smaller antiferromagnetic contribution than in **2** and **3** (Fig. 6).

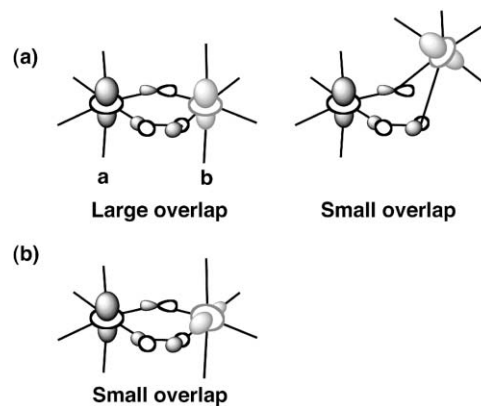


Fig. 6 Effect of the τ angle on the overlap between magnetic orbitals ϕ_a and ϕ_b for collinear (a, complexes **2** and **3**) and non-collinear (b, complex **1**) arrangements.

For **1**, the orbital overlap between two z^2 orbitals through the oxo and oximate bridges have different signs—positive overlap between the z^2 orbital of atom **b** with the p orbital of the oxo bridging ligand, but negative with the p orbital of the oxygen atom of the oximate ligand. This results in a small total overlap value (Fig. 6b). The sign is the same for complexes **2** and **3** (Fig. 6a) giving a larger antiferromagnetic contribution—according to the Kahn–Briat model.³² Thus, we can conclude that both the structural distortion (τ angle) and the different arrangement of the Jahn–Teller play a significant role in the differences observed in the magnetic behaviour of **1–3**.

However, one has to remember that the DFT calculations have been performed on dinuclear models that impede a quantitative estimation of both the countercomplementarity phenomenon and the structural distortion of the $\{Mn_3O(NO)_3\}$ core (τ dihedral angle). In fact, the rigidity of the salicylaldoximate ligand prevents a forced planarity of the $\{Mn_3O(NO)_3\}$ core; hence the reason for employing a model ligand with larger flexibility. From the experimental molecular geometry of **3** and replacing

the salicylaldoximate ligand with a formaldoximate ligand and a water molecule (Fig. 7), we have built models **3a** and **3b**. Model **3a** is equivalent to the experimental complex **3**, whereas **3b** is built from **3a** by flattening the $\{\text{Mn}_3\text{O}(\text{NO})_3\}$ core (*i.e.* all atoms in the magnetic core are placed on the same plane), with all bond lengths preserved. In this instance DFT calculations using the B3LYP functional provide the following results: $J_a = -11.3 \text{ cm}^{-1}$ and $J_b = -15.6 \text{ cm}^{-1}$ for **3a** and $J_a = -8.4 \text{ cm}^{-1}$ and $J_b = -17.9 \text{ cm}^{-1}$ for **3b**. The results show that, as expected, the antiferromagnetic J_b coupling is weakened when a loss of the planarity in the $\{\text{Mn}_3\text{O}(\text{NO})_3\}$ core occurs. A change in the magnitude of the J_a constant is also observed when we move from model **3a** to **3b**. This change is the opposite to that observed for J_b . This result gives some credence to the countercomplementarity phenomenon; the cancellation of the contribution from each of the bridging ligands involved in the magnetic coupling can be increased or decreased when structural changes are applied. This is supported by models **3a2** and **3b2** that have been built from models **3a** and **3b**, respectively, by replacing the carboxylate ligands by water molecules. Similar conclusions are obtained when we move from model **3a2** to **3b2** ($J_a = -16.1 \text{ cm}^{-1}$ and $J_b = -15.5 \text{ cm}^{-1}$ for **3a2** and $J_a = -17.7 \text{ cm}^{-1}$ and $J_b = -19.7 \text{ cm}^{-1}$ for **3b2**). Here, since the J_a and J_b magnetic couplings are more equivalent, the magnitude and changes in this constant are similar. Even when the carboxylate pathway is removed, these last models display much larger J_a constants than their precedent models, allowing us to conclude that the countercomplementarity effect has indeed an influence on the magnitude of the magnetic coupling in these complexes.

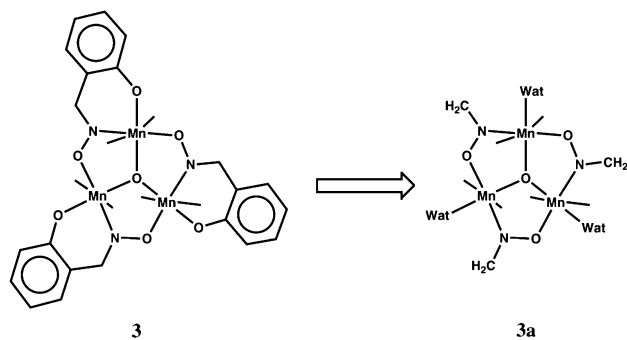


Fig. 7 Schematic view showing models **3** and **3a**.

Conclusions

It is likely that in the problem presented here (like in many scientific problems) there is no simple “black and white” conclusion. The DFT study has suggested that the oxime twist angle and the alignment of the Jahn–Teller axes are important factors, but that several factors are at play. For example, the weakening of the AF exchange *via* the oxide’s displacement from the Mn_3 plane. What we need to do now is deconvolute the problem step by step. This is the initial stage the present DFT studies attempt to address. In a next step we plan to perform DFT studies on a larger family of Mn_3 complexes that includes experimentally obtained examples where the central oxide is in the Mn_3 plane in conjunction with analogues where the oxide is progressively forced out of the Mn_3 plane. However, we accept it will be a difficult challenge to build

models with different dihedral angles in which the bond lengths and geometrical parameters are preserved. What is clear from this preliminary work is that we need more compounds to evaluate the relative importance of the various factors involved. We are working towards this direction.

Literally hundreds of beautiful polymetallic clusters of Mn^{III} ions with fascinating magnetic properties—including high-spin molecules and single-molecule magnets—have been built from simple triangular building blocks. These, with few exceptions, are based on the antiferromagnetic Mn^{III} carboxylates, $[\text{Mn}^{\text{III}}_3\text{O}(\text{O}_2\text{CR})_6\text{L}_3]^+$. The isolation of analogous ferromagnetic triangles, $[\text{Mn}_3\text{O}(\text{oxime})_3(\text{O}_2\text{CR})_{3-n}\text{L}_{n+1}]$, ($\text{L} = \text{py}, \text{H}_2\text{O}$ *etc.*) clearly adds much potential to this synthetic scheme and perhaps promises a route to polymetallic clusters with larger spin ground states and enhanced SMM behaviour. Here we have shown that small structural distortions— τ angles and the orientation of Jahn–Teller axes—play a significant role in the switching of antiferromagnetic exchange to ferromagnetic exchange. Harnessing these changes in a controllable way in the synthesis of larger polymetallic clusters is the next, and undoubtedly difficult, challenge.

Acknowledgements

The research reported was supported by the Dirección General de Investigación del Ministerio de Educación y Ciencia and Comissió Interdepartamental de Ciència i Tecnologia (CIRIT) through grants CTQ2005–08123–C02–02/BQU and 2005SGR–00036, respectively. The authors thankfully acknowledge the computer resources, technical expertise and assistance provided by the Barcelona Supercomputing Center (Centro Nacional de Supercomputación) and Centre de Supercomputació de Catalunya. T. C. thanks the Ministerio de Educación y Ciencia for a PhD grant. E. K. B. thanks the EPSRC and Leverhulme Trust (UK). S. P. P. thanks PYTHAGORAS I (Greece), and G. C. acknowledges the NSF (USA).

Notes and references

- (a) Th. C. Stamatatos, D. Foguet-Albiol, C. C. Stoumpos, C. P. Raptopoulou, A. Terzis, W. Wernsdorfer, S. P. Perlepes and G. Christou, *J. Am. Chem. Soc.*, 2005, **127**, 15380; (b) Th. C. Stamatatos, D. Foguet-Albiol, S.-C. Lee, C. C. Stoumpos, C. P. Raptopoulou, A. Terzis, W. Wernsdorfer, S. O. Hill, S. P. Perlepes and G. Christou, *J. Am. Chem. Soc.*, 2007, **129**, 9484.
- R. D. Cannon and R. P. White, *Prog. Inorg. Chem.*, 1988, **36**, 195.
- R. D. Cannon, U. A. Jayasooriya, R. Wu, S. K. arapKoske, J. A. Stride, O. F. Nielsen, R. P. White, G. J. Kearley and D. J. Summerfields, *J. Am. Chem. Soc.*, 1994, **116**, 11869 and references therein.
- C. J. Milios and E. K. Brechin, *Polyhedron*, 2007, **26**, 1927.
- (a) C. J. Milios, A. Vinslava, P. A. Wood, S. Parsons, W. Wernsdorfer, S. P. Perlepes, G. Christou and E. K. Brechin, *J. Am. Chem. Soc.*, 2007, **129**, 8; (b) C. J. Milios, A. Vinslava, A. Whittaker, S. Parsons, W. Wernsdorfer, S. P. Perlepes, G. Christou and E. K. Brechin, *Inorg. Chem.*, 2006, **45**, 5272; (c) C. J. Milios, C. P. Raptopoulou, A. Terzis, F. Lloret, R. Vicente, S. P. Perlepes and A. Escuer, *Angew. Chem., Int. Ed.*, 2004, **43**, 210.
- A. D. Becke, *Phys. Rev. A.*, 1988, **38**, 3098.
- C. T. Lee, W. T. Yang and R. G. Parr, *Phys. Rev. B.*, 1988, **37**, 785.
- A. D. Becke, *J. Chem. Phys.*, 1993, **98**, 5648.
- M. J. Frisch, G. W. Trucks, H. B. Schlegel, G. E. Scuseria, M. A. Robb, J. R. Cheeseman, J. J. A. Montgomery, T. Vreven, K. N. Kudin, J. C. Burant, J. M. Millam, S. S. Iyengar, J. Tomasi, V. Barone, B. Mennucci, M. Cossi, G. Scalmani, N. Rega, G. A. Petersson, H. Nakatsuji, M. Hada, M. Ehara, K. Toyota, R. Fukuda, J. Hasegawa, M. Ishida, T. Nakajima, Y. Honda, O. Kitao, H. Nakai, M. Klene, X. Li,

- J. E. Knox, H. P. Hratchian, J. B. Cross, V. Bakken, C. Adamo, J. Jaramillo, R. Gomperts, R. E. Stratmann, O. Yazyev, A. J. Austin, R. Cammi, C. Pomelli, J. W. Ochterski, P. Y. Ayala, K. Morokuma, G. A. Voth, P. Salvador, J. J. Dannenberg, V. G. Zakrzewski, S. Dapprich, A. D. Daniels, M. C. Strain, O. Farkas, D. K. Malick, A. D. Rabuck, K. Raghavachari, J. B. Foresman, J. V. Ortiz, Q. Cui, A. G. Baboul, S. Clifford, J. Cioslowski, B. B. Stefanov, G. Liu, A. Liashenko, P. Piskorz, I. Komaromi, R. L. Martin, D. J. Fox, T. Keith, M. A. Al-Laham, C. Y. Peng, A. Nanayakkara, M. Challacombe, P. M. W. Gill, B. Johnson, W. Chen, M. W. Wong, C. Gonzalez and J. A. Pople, *Gaussian 03, Revision C.02*, Gaussian, Inc., Wallingford CT, 2004.
- 10 G. B. Bacskay, *Chem. Phys.*, 1981, **61**, 385.
- 11 A. Schäfer, H. Horn and R. Ahlrichs, *J. Chem. Phys.*, 1992, **97**, 2571.
- 12 A. Schäfer, C. Huber and R. Ahlrichs, *J. Chem. Phys.*, 1994, **100**, 5829.
- 13 *Jaguar 6.0*, Schrödinger, Inc., Portland, 2005.
- 14 E. Ruiz, J. Cano, S. Alvarez and P. Alemany, *J. Comput. Chem.*, 1999, **20**, 1391.
- 15 E. Ruiz, S. Alvarez, A. Rodríguez-Fortea, P. Alemany, Y. Paoillon, and C. Massobrio, in *Magnetism: Molecules to Materials*, ed. J. S. Miller, M. Drillon, Wiley-VCH, Weinheim, 2001, vol. II, pp. 5572–5580.
- 16 E. Ruiz, A. Rodríguez-Fortea, J. Cano, S. Alvarez and P. Alemany, *J. Comput. Chem.*, 2003, **24**, 982.
- 17 E. Artacho, J. D. Gale, A. García, J. Junquera, R. M. Martin, P. Ordejón, D. Sánchez-Portal, and J. M. Soler, J. M., In, *SIESTA 1.3*, 2001.
- 18 D. Sanchez-Portal, P. Ordejón, E. Artacho and J. M. Soler, *Int. J. Quantum Chem.*, 1997, **65**, 453.
- 19 E. Artacho, D. Sanchez-Portal, P. Ordejón, A. Garcia and J. M. Soler, *Phys. Status Solidi B*, 1999, **215**, 809.
- 20 J. M. Soler, E. Artacho, J. D. Gale, A. Garcia, J. Junquera, P. Ordejón and D. Sanchez-Portal, *J. Phys.: Condens. Matter*, 2002, **14**, 2745.
- 21 J. Perdew, K. Burke and M. Ernzerhof, *Phys. Rev. Lett.*, 1996, **77**, 3865.
- 22 C. Massobrio and E. Ruiz, *Monatsh. Chem.*, 2003, **134**, 317.
- 23 E. Ruiz, A. Rodríguez-Fortea, J. Tercero, T. Cauchy and C. Massobrio, *J. Chem. Phys.*, 2005, **123**, 074102.
- 24 L. Kleinman and D. M. Bylander, *Phys. Rev. Lett.*, 1982, **48**, 1425.
- 25 N. Trouiller and J. L. Martins, *Phys. Rev. B*, 1991, **43**, 1993.
- 26 S. G. Louie, S. Froyen and M. L. Cohen, *Phys. Rev. B*, 1982, **26**, 1982.
- 27 P. Chaudhuri, E. Rentschler, F. Birkelbach, C. Krebs, E. Bill, T. Weyhermüller and U. Florke, *Eur. J. Inorg. Chem.*, 2003, 541.
- 28 O. Kahn, *Molecular Magnetism*, VCH Publishers, Inc., New York, 1993.
- 29 L. Gutierrez, G. Alzuet, J. A. Real, J. Cano, J. Borrás and A. Castineiras, A., *Inorg. Chem.*, 2000, **39**, 3608–3614.
- 30 P. J. Hay, J. C. Thibeault and R. Hoffmann, *J. Am. Chem. Soc.*, 1975, **97**, 4884.
- 31 G. Christou, S. P. Perlepes, E. Libby, K. Folting, J. C. Huffman, R. J. Webb and D. N. Hendrickson, *Inorg. Chem.*, 1990, **29**, 3657, and references therein.
- 32 O. Kahn and B. Briat, *J. Chem. Soc., Faraday Trans. 2*, 1976, **72**, 268.